JOURNAL OF CHEMICAL & ENGINEERING DATA

ARTICLE

pubs.acs.org/jced

Mixtures of Pyridine and Nicotine with Pyridinium-Based Ionic Liquids

A. B. Pereiro,[†] A. Rodriguez,[‡] M. Blesic,[†] K. Shimizu,[†,§] J. N. Canongia Lopes,*[,†,§] and L. P. N. Rebelo*[,†]

[†]Instituto de Tecnologia Química e Biológica, Universidade Nova de Lisboa, Av. da República 127, 2780-157 Oeiras, Portugal

[‡]Chemical Engineering Department, Vigo University, P.O. Box 36310, Vigo, Spain

[§]Centro de Química Estrutural, Instituto Superior Técnico Universidade de Lisboa (IST/UTL), 1049-001 Lisboa, Portugal

ABSTRACT: The melting temperatures of $[C_n mpy]Cl$ ($4 \leq$ even $n \leq 18$) were determined by a dynamic method and confirmed by differential scanning calorimetry. The latter technique was also used to measure the corresponding enthalpies of fusion. The temperatures marking the onset of decomposition of the eight ionic liquids were determined by thermogravimetry. The solid−liquid and liquid−liquid phase equilibria of binary mixtures of pyridine or nicotine with four ionic liquids of the 1-alkyl-3-methylpyridinium chloride family ($[C_n mpy]Cl$ with $n = 4, 6, 10, 16$) were investigated. The $T-x$ phase diagrams were measured at atmospheric pressure using turbidimetry in the (280 to 378) K temperature range. The diagrams show that pyridine is miscible in all proportions with the four studied ionic liquids while nicotine is only partially miscible with $[C_4mpy]Cl$ and $[C_6mpy]Cl$. Data were interpreted using molecular dynamics simulations. The study illustrates, once again, the unique structural and solvent properties of ionic liquids.

INTRODUCTION

Mixtures of ionic liquids and aromatic molecules exhibit interesting and unusual phase equilibria such as liquid−liquid demixing upon temperature increase,[1,2] liquid clathrate formation,[3] solid−liquid equilibria (SLE) with inclusion crystal structures,[4−6] and enhanced solubility of the aromatic compounds in the ionic liquid as compared to that of aliphatic solutes.[2] These features led to several applications in either extraction recipes—for instance, of alkaloids such as nicotine or caffeine[7]—or reaction processes.[8−16]

Different pieces of evidence can help explain these properties. For instance, benzene, toluene, and α-methylstyrene diluted in bis(trifluoromethylsulfonyl)imide-based ILs exhibit activity coefficients that increase with increasing temperature[17−19] for the low alkyl chained ILs, thus imposing exothermic conditions as a minimum requisite for causing high temperature demixing phenomena. From a molecular point of view these aromatic solvents must be able to form hydrogen bonds or other specific, oriented interactions with the ions that compose the ionic liquids. Those interactions, along with the pervasive electrostatic forces, will be responsible for the unusual phase behavior.[20] In addition, it is known[21] that ionic liquids are characterized by a doubly dual nature expressed on the one hand by the existence of polar and nonpolar domains[22] and, on the other, by distinctive interactions of any solute with the anions or the cations that constitute the ionic media. This unique nature provides them with good solvent quality for both polar and nonpolar substances. In the case of mixtures of ionic liquids with aromatic molecules, the interactions between the electric dipole and the quadrupole moments of the latter species and the polar/nonpolar or cation/anion domains of the former can explain the complex solubility trends found for the solubility of fluorinated benzene species in a given ionic liquid.[23] The fact that pyridine (where the presence of an heteroatom in the aromatic ring confers it a sizable electric dipole moment) is generally more soluble than benzene in many ionic liquids can also be rationalized along the same lines and contributes to the idea that ionic liquids are good candidates to extract and purify pyridine derivatives, such as nicotine.[2,7]

Our group has accumulated knowledge on both the physical properties of pyridinium NTf_2-based ionic liquids[24] and on their mixtures with water.[25]

In this paper we evaluate the use of ionic liquids belonging to the 1-alkyl-3-methylpyridinium chloride series, $[C_n mpy]Cl$ with $n = 4, 6, 10$, and 16, as solvents for pyridine and nicotine. This particular ionic liquid family was chosen taking into account that the *N*-alkylpyridinium cation is also a derivative of pyridine. The corresponding $T-x$ phase diagrams were determined by monitoring cloud-point temperature data under solid−liquid and, when present, liquid−liquid equilibrium (LLE) conditions.

The melting point temperatures (T_{mp}), molar enthalpies of fusion (ΔH_{fus}), and the onset-of-decomposition temperatures (T_{onset}) were also determined by differential scanning calorimetry (DSC) and thermogravimetric analysis (TGA) for an extended set of pure $[C_n mpy]Cl$ ionic liquids, with $n = 4, 6, 8, 10, 12, 14, 16$, and 18.

EXPERIMENTAL SECTION

Materials. The $[C_n mpy]Cl$ ionic liquids ($n = 4, 6, 8, 10, 12, 14, 16$, and 18) were all synthesized and purified at the QUILL Centre, Belfast using standard published procedures.[26] The analyses by NMR of the obtained products confirmed impurity levels lower than 1 % (mole fraction) in all cases. Prior to their use, all ionic liquids were dried under vacuum ($P = 0.1$ Pa) for

Special Issue: Kenneth N. Marsh Festschrift

Received: February 18, 2011
Accepted: June 7, 2011
Published: June 23, 2011

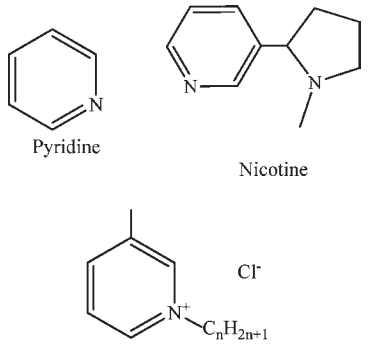

Figure 1. Schematic molecular structure of pyridine, nicotine, and *N*-alkyl-3-methylpyridinium chloride ionic liquids, [C$_n$mpy]Cl.

several days at moderate temperature (T = 333 K) to remove water and any trace of organic solvent. Karl Fisher titration have shown water contents in the (400 to 700) ppm (mass) range, a value deemed acceptable for this series of hydrophilic ionic liquids. Pyridine and nicotine were supplied by Sigma-Aldrich with purities of ≥ 99.9 % and ≥ 99 %, respectively. The chemicals were kept under nitrogen atmosphere and protected from light. Before the measurements, pyridine and nicotine were dried using 3 Å molecular sieves. Figure 1 shows the structure of the chemicals used in this work.

Methods. Temperatures and enthalpies of fusion of the pure [C$_n$mpy]Cl ionic liquids were measured by differential scanning calorimetry (DSC), using a modulated calorimeter (TA Instruments, model 2920). Cooling was accomplished by using a refrigerated cooling system capable of controlling the temperature down to 220 K. The heating/cooling regime was adjusted for each sample separately. Typically, a standard heating and cooling ramp of 5 K·min^{-1} was used. Both the onset and the peak melting temperatures were measured, and the enthalpy of fusion was determined by integration of the experimental heat flow curves as functions of temperature. Dry nitrogen at a flow rate of about 20 cm^3·min^{-1} was used as the purge gas of the DSC cell. Temperatures of fusion were also determined using a dynamic method where the samples were slowly heated 0.5 K·min^{-1} in small glass vials until the disappearance of the last crystal was observed. In this case, the uncertainty of the melting point temperatures (± 1 K in most cases) is much greater than that of measurements in the DSC cell (± 0.2 K in most cases). The uncertainty associated with the determination of the enthalpies of fusion using the present technique and samples was estimated to be ± 3 kJ·mol^{-1}.

Decomposition temperature measurements were performed in a thermogravimetric analyzer (TA Instruments, model Q50). The experiments were performed at atmospheric pressure in platinum pans with heating rates of 10 K·min^{-1}. The onset of the weight loss in each thermogram was used as a measure of the decomposition temperature.

The SLE and LLE conditions were determined using a dynamic method with visual detection of the phase transition: in the case of SLE this corresponded to the temperature at which the last crystal disappears as the temperature of the mixture is increased; in the case of the LLE, the demixing temperature is determined when the temperature of the heterogeneous mixture is increased and the last sign of turbidity disappears. Mixtures were prepared by gravimetry using an analytical high-precision balance with ± 0.01 mg resolution (Precisa, model 40SM-200A) in narrow sealed Pyrex glass vials equipped with stirring. The vials were placed in a thermostatic bath filled with ethanol (T = (253 to 300) K) or silicon oil (T = (300 to 473) K). The temperature was monitored using a four-wire platinum resistance thermometer coupled to a multimeter (Keithley 199 System DMM/Scanner). The temperature accuracy was ± 0.05 K, while the overall uncertainty of the transition temperature measurements is obviously greater than the instrumental error and is estimated to be ± 1 K.

Table 1. Melting Point Temperature, T_{mp}, Molar Enthalpy of Fusion, $\Delta_s^l H_m$, and Decomposition Onset Temperature, T_{onset}, of Eight *N*-Alkyl-3-methylpyridinium Chloride Ionic Liquids, [C$_n$mpy]Cl[a]

	T_{mp}/K		$\Delta_s^l H_m$/kJ·mol^{-1}	T_{onset}/K
Component	Dynamic	DSC	DSC	TGA
[C$_4$mpy]Cl	383	384.5	28	515
[C$_6$mpy]Cl	353	355.1	20	511
[C$_8$mpy]Cl	352	353.2	15	505
[C$_{10}$mpy]Cl	349	352.5	14	500
[C$_{12}$mpy]Cl	360	360.8	37	500
[C$_{14}$mpy]Cl	368	366.8	43	500
[C$_{16}$mpy]Cl	383	383.0	40	501
[C$_{18}$mpy]Cl	386	385.4	28	501

[a] The uncertainty associated with each determination is ± 1 K (T_{mp}, dynamic), ± 0.2 K (T_{mp}, DSC), ± 3 kJ ($\Delta_s^l H_m$, DSC), and ± 3 K (T_{onset}, TGA).

Molecular Dynamics Simulations. The molecular force field used to represent the [C$_4$mpy]Cl and [C$_{10}$mpy]Cl ionic liquids and the pyridine solute is based on the optimized potentials for liquid simulations all atoms (OPLS-AA) model[27] with additional parameters specified by the Canongia Lopes and Pádua (CLP) force field:[28] the chloride anion has been described in the third part of a sequence of articles concerning the application of the CLP force field to different ionic liquid ions and their homologous series,[29] whereas the [C$_n$mpy]$^+$ cations have been modeled using an extended version of the CLP force field.[30]

The pure ionic liquids, [C$_4$mpy]Cl and [C$_{10}$mpy]Cl, and four solutions of pyridine either in [C$_4$mpy]Cl or in [C$_{10}$mpy]Cl were studied at 473 K. All simulations were performed using molecular dynamics, implemented using the DL_POLY code.[31] Starting from low-density initial configurations, systems composed of 200 ionic liquid ion pairs and mixtures containing 10 or 40 molecules of pyridine in 200 ionic liquid ion pairs were equilibrated under constant NpT conditions for 500 ps at 473 K (Nosé-Hoover thermostat and barostat with time constants of 0.5 and 2 ps, respectively). The final density was attained after about 50 ps. Further consecutive simulation runs of 100 ps each were used to produce equilibrated systems at the studied temperatures. A total of 12 such runs have been considered at this stage, implying an overall simulation time (including equilibration) of around 1.8 ns. Three intermediate charge and temperature annealing sequences have also been introduced between the successive production runs to confirm that the system would return to its equilibrium state. Repulsive, dispersive, and electrostatic interactions were calculated explicitly for cutoff distances shorter than 1.6 nm and estimated using long-range corrections for distances larger than

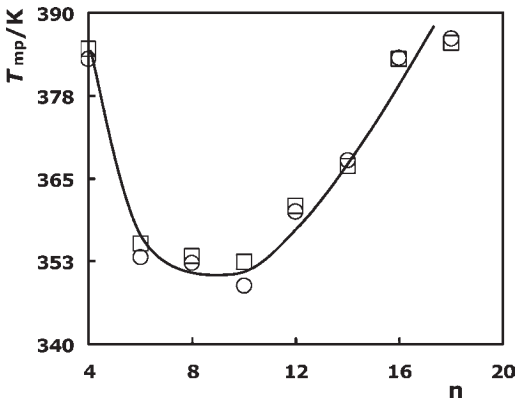

Figure 2. Melting point temperature, T_{mp}, as a function of the number of carbon atoms in the alkyl side chain, n, of [$C_n$mpy]Cl ionic liquids: □, DSC data; ○, dynamic method data. The solid line is merely a guide for the eye.

Table 2. Experimental SLE Temperatures, T^{SLE}, versus Mole Fraction x_1, for {[Cnmpy]Cl (1) + Pyridine (2)}[a]

x_1	T^{SLE}/K	x_1	T^{SLE}/K	x_1	T^{SLE}/K
		{[C_4mpy]Cl (1) + Pyridine (2)}			
0.0834	296.8	0.3861	334.6	0.6998	366.5
0.1536	306.3	0.4759	346.5	0.8542	375.1
0.2280	315.9	0.5815	356.4	0.9607	380.0
0.3014	325.5				
		{[C_6mpy]Cl (1) + Pyridine (2)}			
0.2363	279.4	0.4729	311.7	0.7639	332.8
0.3124	289.2	0.5525	317.2	0.8957	342.1
0.3980	300.1	0.6485	325.8	0.9632	350.2
		{[C_{10}mpy]Cl (1) + Pyridine (2)}			
0.1885	286.3	0.4060	317.7	0.7483	341.2
0.2487	295.5	0.4918	325.3	0.8558	343.6
0.2822	302.2	0.5860	333.0	0.9522	345.4
0.3452	308.6	0.6620	337.0		
		{[C_{16}mpy]Cl (1) + Pyridine (2)}			
0.0064	295.4	0.1155	324.6	0.4576	368.5
0.0118	299.7	0.1451	330.7	0.5084	371.0
0.0209	304.2	0.2283	349.5	0.5733	372.6
0.0360	310.0	0.2907	358.3	0.7406	377.7
0.0471	312.1	0.3582	363.0	0.8596	381.9
0.0795	318.4				

[a] The uncertainty in the two quantities are ± 1 K (T^{SLE}) and ± 0.0008 (x_1).

the cutoff. In the case of electrostatic interactions, the Ewald summation method with six reciprocal-space vectors was used. Finally, 1000 configurations were stored from production runs of 300 ps, to obtain statistical meaningful radial distribution functions between selected atom pairs.

RESULTS AND DISCUSSION

Properties of Pure [$C_n$mpy]Cl Ionic Liquids. The melting point temperatures (T_{mp}), molar enthalpies of fusion (ΔH_{fus}), and the onset-of-decomposition temperatures (T_{onset}) of pure [$C_n$mpy]Cl ionic liquids, with n = 4, 6, 8, 10, 12, 14, 16, and 18, are presented in Table 1.

Table 3. Experimental SLE and LLE Temperatures, T^{SLE} and T^{LLE}, versus Mole Fraction x_1, for {[$C_n$mpy]Cl (1) + Nicotine (2)}

x_1	T^{SLE}/K	T^{LLE}/K	x_1	T^{SLE}/K	T^{LLE}/K
		{[C_4mpy]Cl (1) + Nicotine (2)}			
0.0037	364.2	389.2	0.4674	364.6	
0.0788	364.4		0.5781	364.4	400.6
0.1463	364.2		0.6125	366.0	384.0
0.2206	364.7		0.7873	371.9	
0.3509	364.3		0.9180	377.6	
		{[C_6mpy]Cl (1) + Nicotine (2)}			
0.0036	314.2		0.4788	335.3	368.9
0.0093	333.6	389.2	0.5038	336.0	359.7
0.0098	333.7	419.8	0.5347	336.1	351.6
0.1128	334.8		0.5802	337.3	345.3
0.2017	335.1		0.6687	340.2	
0.2670	335.1		0.7177	341.1	
0.3904	334.4		0.8206	342.8	
0.4412	334.4	392.0	0.9236	349.0	
		{[C_{10}mpy]Cl (1) + Nicotine (2)}			
0.0701	293.1	0.2446	311.6	0.5761	331.3
0.1071	297.6	0.3101	315.0	0.6727	334.5
0.1448	301.3	0.3506	318.2	0.7880	338.5
0.1719	304.4	0.4103	320.5	0.8794	341.9
0.2029	307.2	0.4949	325.7	0.9576	344.0
		{[C_{16}mpy]Cl (1) + Nicotine (2)}			
0.0148	311.4	0.1152	329.2	0.5188	360.2
0.0203	312.2	0.1450	335.9	0.6034	362.1
0.0280	313.9	0.1850	345.8	0.6683	367.3
0.0392	315.1	0.2465	350.1	0.6992	369.6
0.0538	317.7	0.3381	352.8	0.7510	371.6
0.0774	323.4	0.4342	356.7	0.8218	372.6

The melting point temperatures of each ionic liquid are plotted in Figure 2 as a function of the alkyl chain length of the 1-alkyl-3-methylpyridinium cation. The nonmonotonous ("U" shape) behavior of the function is similar to that already found for ionic liquids based on the 1-alkyl-3-methylimidazolium cation.[32]

In the case of ionic liquids the onset of thermal decomposition is an issue of particular importance and practical significance. Since these compounds have negligible vapor pressures at or near ambient temperatures,[33,34] their potential operating liquid range is not limited by their normal boiling or critical temperatures but by the temperatures at which they start to thermally decompose.[35] Thus, the ionic liquids studied in this work—with T_{onset} values in the (500 to 515) K range—exhibit operating liquid ranges larger than 100 K (up to 150 K for those ionic liquids with lower melting point temperatures). These T_{onset} values are comparable to those of other classes of ionic liquids (namely, those based on the more commonly used dialkylimidazolium cation), where decomposition temperatures around (450 to 500) K and liquid

dx.doi.org/10.1021/je2001446 |J. Chem. Eng. Data 2011, 56, 4356–4363

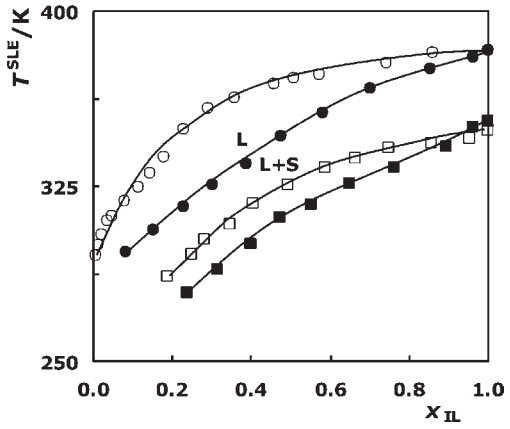

Figure 3. Experimental SLE temperature, T^{SLE}, as a function of composition expressed as ionic liquid mole fraction, x_{IL}, for {[$C_n$mpy]Cl (1) + pyridine (2)} binary mixtures: ●, n = 4; ■, n = 6; □, n = 10; ○, n = 16. The solid lines are just guides to the eye representing the boundary between the regions of one phase (liquid solution, L) and two phases (saturated liquid solution and pure ionic liquid solid, L+S). The different regions are labeled in the graphic for the solutions based on the [C_4mpy]Cl ionic liquid (●).

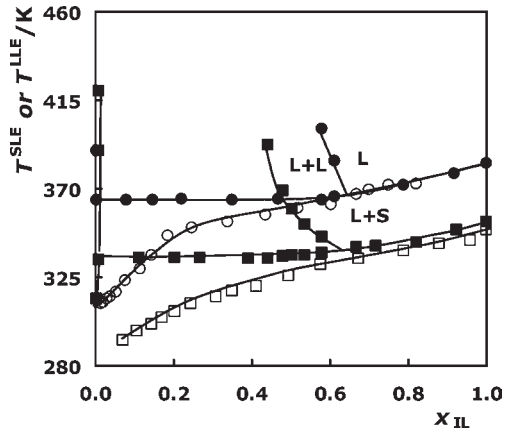

Figure 4. Experimental SLE and LLE temperatures, T^{SLE} and T^{LLE}, as a function of composition expressed as ionic liquid mole fraction, x_{IL}, for {[$C_n$mpy]Cl (1) + nicotine (2)} binary mixtures: ●, n = 4; ■, n = 6; □, n = 10; ○, n = 16. The solid lines are just guides to the eye representing the boundary between the regions of one phase (liquid solution, L), two liquid phases (ionic liquid rich phase and almost pure nicotine, L+L) and one liquid plus one solid phases (saturated liquid solution plus ionic liquid solid, L+S). The different regions are labeled in the graphic for the solutions based on the [C_4mpy]Cl ionic liquid (●).

ranges of almost 200 K are quite common. In this context, the most conspicuous characteristic of the present data refers to the relatively high decomposition temperatures found for chloride-based ionic liquids.

Phase Equilibria of ([$C_n$mpy]Cl + Pyridine/Nicotine) Binary Mixtures. Phase equilibria data for ([$C_n$mpy]Cl + pyridine) and ([$C_n$mpy]Cl + nicotine) binary mixtures with n = 4, 6, 10, and 16 are presented in Tables 2 and 3, respectively. The tables include SLE and LLE transition temperatures, T^{SLE} and T^{LLE}, as a function of composition expressed in ionic liquid mole fraction. The data are also plotted in Figures 3 (pyridine systems), 4 (nicotine systems), and 5 (comparison of all systems).

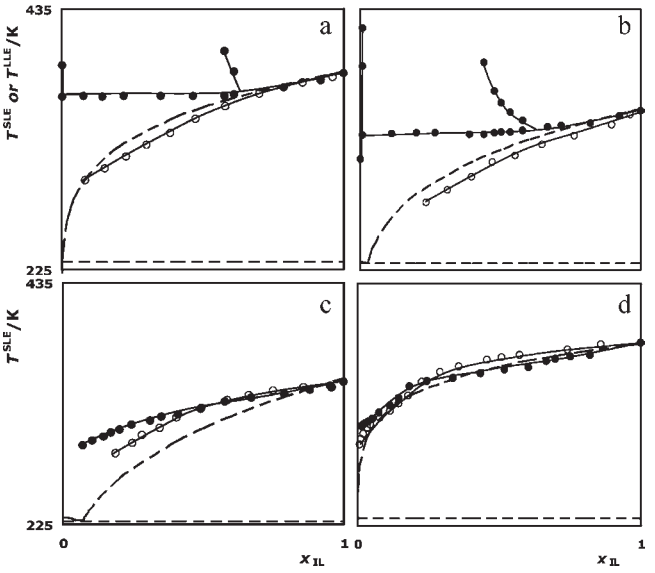

Figure 5. Experimental SLE and LLE temperature, T^{SLE} and T^{LLE}, as a function of composition expressed as ionic liquid mole fraction, x_{IL}, for {[$C_n$mpy]Cl (1) + pyridine (2)} (open symbols) and {[$C_n$mpy]Cl (1) + nicotine (2)} (full symbols) binary mixtures. Solid lines are only guides to the eye, and dashed lines represent the ideal solubility of ionic liquid in pyridine, calculated from their molar enthalpy and temperature of fusion values.[36] (a) [C_4mpy]Cl systems; (b) [C_6mpy]Cl; (c) [C_{10}mpy]Cl; (d) [C_{16}mpy]Cl.

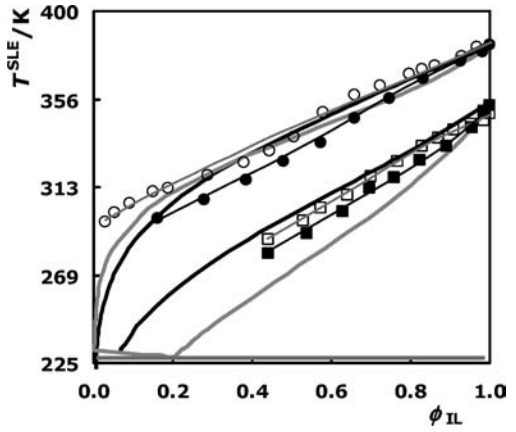

Figure 6. Experimental SLE temperature, T^{SLE}, as a function of composition expressed as ionic liquid volume fraction, ϕ_{IL}, for {[$C_n$mpy]Cl (1) + pyridine (2)} binary mixtures: ●, n = 4; ■, n = 6; □, n = 10; ○, n = 16. The thin solid lines are only guides to the eye, and the wide black (n = 4 and 6) and gray (n = 10 and 16) solid lines represent the ideal solubility.

The ([$C_n$mpy]Cl + pyridine) systems exhibit complete miscibility of the two components in the liquid phase. On the other hand the SLE are described by the four liquidus lines shown in Figure 3. These lines suggest that it is possible to group the SLE trends into two pairs of systems: ([C_4mpy]Cl + pyridine) with ([C_{16}mpy]Cl + pyridine) and ([C_6mpy]Cl + pyridine) with ([C_{10}mpy]Cl + pyridine). However, this arrangement is just a consequence of the nonmonotonous behavior of the melting point temperatures of the four ionic liquids: T_{mp}([C_4mpy]Cl) ≈ T_{mp}([C_{16}mpy]Cl) > T_{mp}([C_6mpy]Cl) ≈ T_{mp}([C_{10}mpy]Cl).

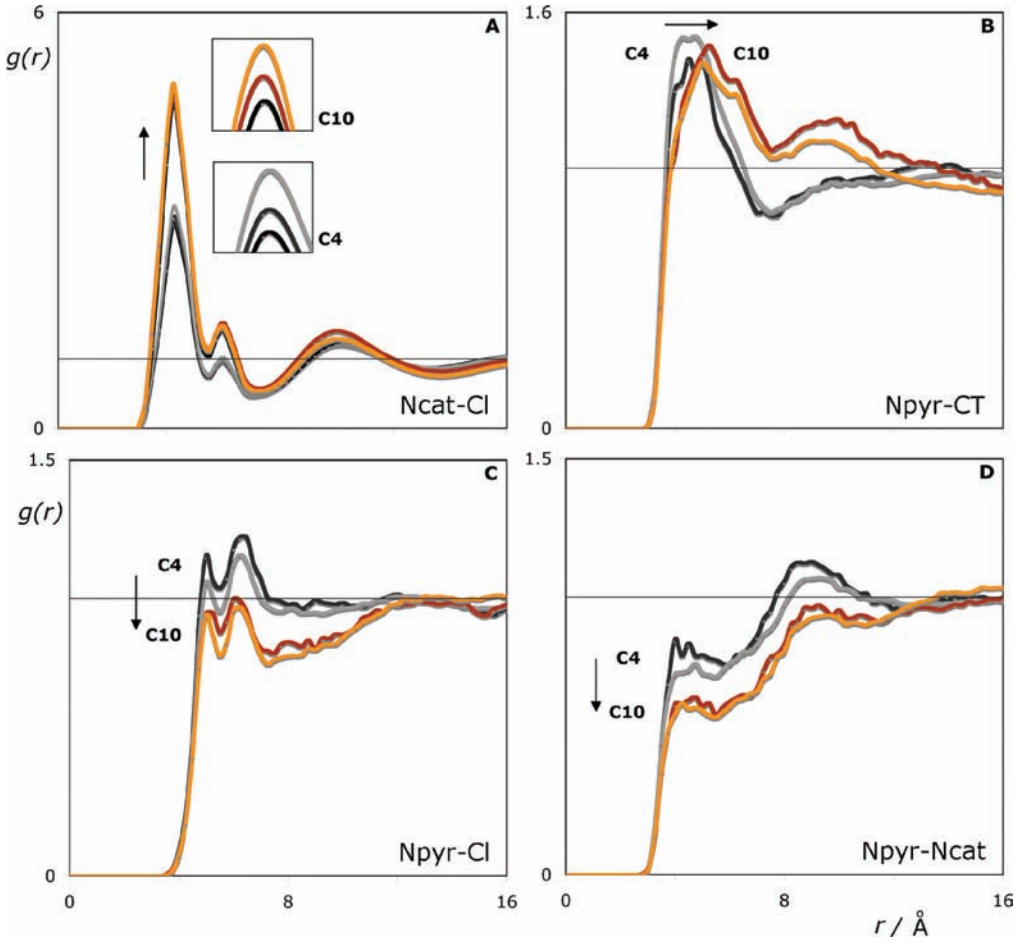

Figure 7. Radial distribution functions (rdfs) obtained from molecular dynamic runs in simulation boxes of pure $[C_4mim]Cl$ and $[C_{10}mim]Cl$ with 400 ions (C4 and C10 black lines in panel A) and mixtures of $[C_4mim]Cl$ and $[C_{10}mim]Cl$ (400 ions) with 10 and 40 pyridine molecules (dark and light gray in C4 mixtures; dark and light orange in C10 mixtures). All rdfs are between the atom types displayed in each panel. A: anion−cation rdfs showing the increase of segregation between the polar network and the nonpolar domains as one increases the size of the latter by the shift from C4 to C10; B: pyridine−nonpolar domain (alkyl chain terminal carbon, CT) rdfs showing the "sinking" of the pyridine molecules in the larger nonpolar domains of $[C_{10}mim]Cl$—larger Npyr-CT distances corresponding to roomier nonpolar domains; C and D: pyridine−anion and pyridine−cation rdfs showing more efficient interactions between pyridine and both ions when mixed in $[C_4mim]Cl$ (and solvated in smaller nonpolar domains).

In fact the SLE trends of all systems are quite standard, with the liquidus lines starting at the melting point temperatures of each pure ionic liquid and following the usual pattern of freezing point depression, $\Delta T_{mix} = T_{mp}([C_n mpy]Cl) - T_{mix}$, as pyridine is added to the mixture:

$$\Delta T_{mix} = x_{pyr} R (T_{mp}([C_n mpy]Cl))^2 / \Delta_{fus} H_m([C_n mpy]Cl) \quad (1)$$

From the data collected in Table 1, it was possible to estimate the ideal solubility lines of pyridine in the different ionic liquids. Conversely, the ideal solubility lines of the ionic liquids in pyridine were also estimated, taking into account the melting point temperature of pyridine ($T_{mp}(C_5H_5N) = 232$ K)[36] and its enthalpy of fusion ($\Delta_{fus}H_m(C_5H_5N) = 8.28$ kJ·mol^{-1}).[36] These ideal trends are represented in Figure 5 along with the real liquidus lines. The most obvious feature of the former lines is that due to the large differences between the melting points of the $[C_n mpy]Cl$ ionic liquids and pyridine, the ideal eutectic temperature will be only slightly lower than the melting temperature of pyridine and the eutectic composition not far removed from pure pyridine. Due to limitations of the experimental methods used, it was not possible to determine directly the existence of such eutectics. Nevertheless, the ideal solubility lines explain the monotonous behavior of the measured liquidus lines. Moreover, the slopes of the ideal and liquidus lines (that according to eq 1 should be directly proportional to T_{mp}^2 and inversely proportional to $\Delta_{fus}H_m$) are quite close, except in the case of the system with $[C_{10}mpy]Cl$. In this case the difference can be explained by the low value of $\Delta H_{fus,[C_{10}mpy]Cl}$ (the lowest of the four ionic liquids used in the mixtures) that contributes to a quite high slope of the ideal solubility line. In fact the liquidus lines corresponding to the mixtures with ionic liquids with larger alkyl side chains in the cations ($[C_{10}mpy]^+$ and $[C_{16}mpy]^+$) exhibit lower slopes than those of the mixtures that include ionic liquids with smaller cations ($[C_4mpy]^+$ and $[C_6mpy]^+$). These comparisons are quite straightforward if one compares the pairs (C4 and C16) and (C6 and C10), where in each case the liquidus lines start at approximately the same melting point temperatures. However, it must be stressed that the less steep and more curved liquidus curves of the systems containing $[C_{10}mpy]^+$ and $[C_{16}mpy]^+$ are caused by the larger difference between the molar volumes of the

dx.doi.org/10.1021/je2001446 |J. Chem. Eng. Data 2011, 56, 4356–4363

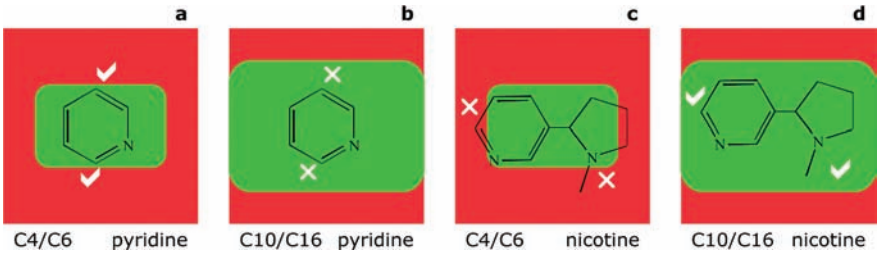

Figure 8. Goldilocks-type schematics of the solvation process of pyridine and nicotine in [$C_n$mim]Cl ionic liquids. a: enhanced stability/solubility of pyridine in C4/C6 "just-right" nonpolar domains with strong interactions with the polar network (check signs); b: decreased stability of pyridine in C10/C16 "too big" nonpolar domains with weak interactions with the polar network (X-marks); c: LLE of nicotine in C4/C6 "too small" nonpolar domains (X-marks); d: complete miscibility of nicotine in C10/C16 "just right" nonpolar domains (check marks).

corresponding ionic liquids and pyridine. If Figure 3 is redrawn in terms of volume fraction instead of mole fraction (Figure 6), the slope and curvature of the different liquidus lines is much more similar, although the relation with the corresponding ideal behavior lines (also redrawn in terms of volume fractions) is still the same: positive deviations from the ideal behavior in the case of systems containing the larger cations; negative deviations with smaller cations.

Another way to look at the relative slopes between the different liquidus lines and their relation to the ideal behavior lines is to think about the interactions between pyridine and the ionic liquid (the fact that a volume fraction representation yields a more regular behavior along the homologous series suggests that interactions are indeed a key issue).

For the mixtures of nicotine with the different ionic liquids (Figure 4) the most striking feature is the appearance of liquid−liquid immiscibility regions in the solutions of [C_4mpy]Cl and [C_6mpy]Cl. The two liquid systems that were the more stable with pyridine are now the less stable with nicotine.

As already discussed in the Introduction, pyridine is more soluble than benzene in most ionic liquids because its nitrogen heteroatom confers the molecule a dipole moment that is capable of more efficient interactions with the high charge-density parts of the ions that compose the ionic liquid. Auxiliary molecular dynamics simulations have yielded radial distribution functions that confirm such a notion from a molecular point of view (Figure 7): although a large portion of the pyridine molecule is solvated in the nonpolar domains of the ionic liquid, part of the molecule is oriented toward the vicinity of the polar network, namely, toward the chloride anions. This explains the total miscibility of pyridine in all studied ionic liquids but also why the systems with smaller nonpolar domains have a higher-than-ideal solubility: with a smaller nonpolar-to-polar domain ratio the pyridine molecules can have the best of both worlds, that is, part of the molecule remains solvated in the nonpolar domain while the most acidic hydrogen atoms of the molecule can interact with the chloride atoms of the polar network. When the nonpolar-to-polar ratio increases, the pyridine molecules "plunge" more deeply into the nonpolar domain, and the interactions with the polar network are no longer so efficient (Figure 7, panels B to D). Moreover, the polar network is now more stretched and tightly bound to accommodate the larger (and continuous) nonpolar domain (Figure 7, panel A), which means that part of the chloride atoms are no longer available to interact with the pyridine molecules. In other words, the existence of larger nonpolar regions in the ILs with longer alkyl chain length originates less stable liquid phases with higher solid−liquid transition temperatures.

On the basis of the molecular insights provided by the MD results of the (pyridine + ionic liquid) systems, the following qualitative arguments can be advanced: the difference between pyridine and nicotine is the aliphatic *N*-methylpyrrole group substituted at the 2 position of the former molecule. This large aliphatic residue has to be accommodated in the nonpolar regions of the ionic liquid. When these are too small (as in the case of [C_4mpy]Cl or [C_6mpy]Cl), the systems exhibits liquid−liquid demixing. This effect—smaller alkyl side chains in the cations decrease the solubility and induce the appearance of liquid−liquid immiscibility phenomena—is also found in solutions of imidazolium-based ionic liquids with nicotine[2] or other aromatic[1] and aliphatic molecules.[20,37,38] In the cases where [$C_n$mpy]Cl has a longer alkyl chain length (n = 10 and 16) the fluid phase behavior is similar to the one with pyridine, without the appearance of liquid−liquid demixing.

The different SLE and LLE scenarios found for the eight systems (C4, C6, C10, or C16 with either pyridine or nicotine) are interpreted schematically in Figure 8: in the case of the C4/C6 systems with pyridine the latter molecule fits the nonpolar domains while maintaining at the same time its interactions with the polar network (Figure 8A); in the C10/C16 systems, pyridine sinks more deeply into the larger nonpolar domains, and parts of those favorable interactions are lost (Figure 8B); in the case of nicotine with C4/C6, the molecule does not fit so nicely the nonpolar domains (they get saturated sooner), and this leads to the appearance of liquid−liquid immiscibility for higher concentrations of nicotine (Figure 8C); finally the larger nonpolar domains in C10/C16 are able to accommodate the nicotine molecules, and the stronger van der Waals interactions between the nicotine molecule and the longer alkyl side chains are responsible for the complete miscibility of the two components in the entire concentration range of the mixtures (Figure 8D).

CONCLUSION

The homologous series of 1-alkyl-3-methylpyridinium chloride ionic liquids, [$C_n$mpy]Cl, exhibit working liquid ranges constrained between their melting points ((350 to 390) K) and decomposition temperatures (onset) of about 500 K. These liquid ranges—somewhat shifted to higher temperatures relative to those of their imidazolium-based counterparts—make them good alternative candidates for applications in heterogeneous catalysis or in membrane extraction processes.

Pyridine and nicotine further highlight the unique and tunable solvent properties of ionic liquids: the ratio of polar-to-nonpolar domains in the ionic liquids (that can be easily adjusted by the

length of the alkyl side chains present in most homologous series) determines that [$C_n$mpy]Cl-pyridine mixtures with smaller n (C4 or C6) are more stable than those with greater n (C10, C16), whereas the opposite is true for mixtures containing nicotine—leading to liquid−liquid immiscibility situations in the cases of mixtures with [C_4mpy]Cl or [C_6mpy]Cl.

AUTHOR INFORMATION

Corresponding Author

*E-mail: jnlopes@ist.utl.pt and luis.rebelo@itqb.unl.pt.

Funding Sources

The authors wish to acknowledge the ongoing collaboration with the QUILL research group, Belfast. Financial support to carry out this work was provided by Fundação para a Ciência e Tecnologia (FCT) through projects PTDC/QUIQUI/101794/2008, PTDC/EQU-EQU/102949/2008, and PTDC/QUI/71331/2006. A.B.P. acknowledges Marie Curie Actions, Intra-European Fellowships (IEF) for a contract under FP7-PEOPLE-2009-IEF, 252355, HALOGENILS. K.S. acknowledges the grant SFRH/BPD/38339/2007. The NMR spectrometers are part of the National NMR Network and were purchased in the framework of the National Program for Scientific Re-equipment, contract REDE/1517/RMN/2005, with funds from POCI 2010 (FEDER) and Fundação para a Ciência e a Tecnologia (FCT).

REFERENCES

(1) Łachwa, J.; Szydlowski, J.; Makowska, A.; Seddon, K. R.; Esperança, J. M. S. S.; Guedes, H. J. R.; Rebelo, L. P. N. Changing from an Unusual High-Temperature Demixing to a UCST-Type in Mixtures of 1-Alkyl-3-Methylimidazolium bis{(Trifluoromethyl)Sulfonyl}Amide and Arenes. *Green Chem.* **2006**, *8*, 262–267.

(2) Visak, Z. P.; Lucas, S.; Canongia Lopes, J. N.; Rebelo, L. P. N. Nicotine: On the Potential Role of Ionic Liquids for its Processing and Purification. *J. Phys. Chem. B* **2007**, *111*, 7934–7937.

(3) Surette, J. K. D.; Green, L.; Singer, R. D. 1-Ethyl-3-Methylimidazolium Halogenoaluminate Melts as Reaction Media for the Friedel-Crafts Acylation of Ferrocene. *Chem. Commun.* **1996**, 2753–2754.

(4) Łachwa, J.; Bento, I.; Duarte, M. T.; Canongia Lopes, J. N.; Rebelo, L. P. N. Condensed Phase Behaviour of Ionic Liquid-Benzene Mixtures: Congruent Melting of a [Emim][NTf_2] Center Dot C_6H_6 Inclusion Crystal. *Chem. Commun.* **2006**, 2445–2447.

(5) Deetlefs, M.; Hardacre, C.; Nieuwenhuyzen, M.; Sheppard, O.; Soper, A. K. Structure of Ionic Liquid-Benzene Mixtures. *J. Phys. Chem. B* **2005**, *109*, 1593–1598.

(6) Holbrey, J. D.; Reichert, W. M.; Nieuwenhuyzen, M.; Sheppard, O.; Hardacre, C.; Rogers, R. D. Liquid Clathrate Formation in Ionic Liquid-Aromatic Mixtures. *Chem. Commun.* **2003**, 476–477.

(7) Freire, M. G.; Neves, C. M. S. S.; Marrucho, I. M.; Lopes, J. N. C.; Rebelo, L. P. N.; Coutinho, J. A. P. High-Performance Extraction of Alkaloids using Aqueous Biphasic Systems with Ionic Liquids. *Green Chem.* **2010**, *12*, 1715–1718.

(8) Arce, A.; Earle, M. J.; Heintz, A.; Rodriguez, H.; Seddon, K. R. Separation of Aromatic Hydrocarbons from Alkanes using the Ionic Liquid 1-Ethyl-3-Methylimidazolium bis{(Trifluoromethyl) Sulfonyl} Amide. *Green Chem.* **2007**, *9*, 70–74.

(9) Pereiro, A. B.; Rodriguez, A. Separation of Ethanol-Heptane Azeotropic Mixtures by Solvent Extraction with an Ionic Liquid. *Ind. Eng. Chem. Res.* **2009**, *48*, 1579–1585.

(10) Pereiro, A. B.; Rodriguez, A. Purification of Hexane with Effective Extraction using Ionic Liquid as solvent. *Green Chem.* **2009**, *11*, 346–350.

(11) Pereiro, A. B.; Rodriguez, A. Effective Extraction in Packed Column of Ethanol from the Azeotropic Mixture Ethanol plus Hexane with an Ionic Liquid as Solvent. *Chem. Eng. J.* **2009**, *153*, 80–85.

(12) Pereiro, A. B.; Rodriguez, A. An Ionic Liquid Proposed as Solvent in Aromatic Hydrocarbon Separation by Liquid Extraction. *AIChE J.* **2010**, *56*, 381–386.

(13) Verevkin, S. P.; Ondo, D. Thermodynamic Properties of Mixtures Containing Ionic Liquids. 8. Activity Coefficients at Infinite Dilution of Hydrocarbons, Alcohols, Esters, and Aldehydes in 1-Hexyl-3-Methylimidazolium bis(trifluoromethysulfonyl) Imide using Gas-Liquid Chromatography. *J. Chem. Eng. Data* **2006**, *51*, 434–437.

(14) Letcher, T. M.; Reddy, P. Ternary (Liquid plus Liquid) Equilibria for Mixtures of 1-Hexyl-3-Methylimidazolium (Tetrafluoroborate or Hexafluorophosphate) plus Benzene plus an Alkane at T = 298.2 K and P = 0.1 MPa. *J. Chem. Thermodyn.* **2005**, *37*, 415–421.

(15) Meindersma, G. W.; Podt, G.; de Haan, A. J.; Ternary Liquid-Liquid, A. B. Equilibria for Mixtures of Toluene plus *n*-Heptane plus an Ionic Liquid. *Fluid Phase Equilib.* **2006**, *247*, 158–168.

(16) Arce, A.; Rodriguez, O.; Soto, A. Tert-Amyl Ethyl Ether Separation from its Mixtures with Ethanol using the 1-Butyl-3-Methylimidazolium Trifluoromethanesulfonate Ionic Liquid: Liquid-Liquid Equilibrium. *Ind. Eng. Chem. Res.* **2004**, *43*, 8323–8327.

(17) Krummen, M.; Wasserscheid, P.; Gmehling, J. Measurement of Activity Coefficients at Infinite Dilution in Ionic Liquids using the Dilutor Technique. *J. Chem. Eng. Data* **2002**, *47*, 1411–1417.

(18) Heintz, A.; Kulikov, D.; Verevkin, S. P. Thermodynamic Properties of Mixtures Containing Ionic Liquids. 2. Activity Coefficients at Infinite Dilution of Hydrocarbons and Polar Solutes in 1-Methyl-3-Ethyl-Imidazolium bis(Trifluoromethyl-Sulfonyl) Amide and in 1,2-Dimethyl-3-Ethyl-Imidazolium bis(Trifluoromethyl-Sulfonyl) Amide using Gas-Liquid Chromatography. *J. Chem. Eng. Data* **2002**, *47*, 894–899.

(19) Deenadayalu, N.; Letcher, T. M.; Reddy, P. Determination of Activity Coefficients at Infinite Dilution of Polar and Nonpolar Solutes in the Ionic Liquid 1-Ethyl-3-Methylimidazolium bis(Trifluoromethylsulfonyl) Imidate using Gas-Liquid Chromatography at the Temperature 303.15 or 318.15 K. *J. Chem. Eng. Data* **2005**, *50*, 105–108.

(20) Łachwa, J.; Szydlowski, J.; Najdanovic-Visak, V.; Rebelo, L. P. N.; Seddon, K. R.; da Ponte, M. N.; Esperança, J. M. S. S.; Guedes, H. J. R. Evidence for Lower Critical Solution Behavior in Ionic Liquid Solutions. *J. Am. Chem. Soc.* **2005**, *127*, 6542–6543.

(21) Rebelo, L. P. N.; Canongia Lopes, J. N.; Esperança, J. M. S. S.; Guedes, H. J. R.; Łachwa, J.; Najdanovic-Visak, V.; Visak, Z. P. Accounting for the Unique, Doubly Dual Nature of Ionic Liquids from a Molecular Thermodynamic, and Modeling Standpoint. *Acc. Chem. Res.* **2007**, *40*, 1114–1121.

(22) Canongia Lopes, J. N.; Pádua, A. A. H. Nanostructural Organization in Ionic Liquids. *J. Phys. Chem. B* **2006**, *110*, 3330–3335.

(23) Shimizu, K.; Costa Gomes, M. F.; Pádua, A. A. H.; Rebelo, L. P. N.; Canongia Lopes, J. N. On the Role of the Dipole and Quadrupole Moments of Aromatic Compounds in the Solvation by Ionic Liquids. *J. Phys. Chem. B* **2009**, *113*, 9894–9900.

(24) Oliveira, F. S.; Freire, M. C.; Carvalho, P. I.; Coutinho, J. A. P.; Lopes, J. N. C.; Rebelo, L. P. N.; Marrucho, I. M. Structural and Positional Isomerism Influence in the Physical Properties of Pyridinium NTf_2-Based Ionic Liquids: Pure and Water-Saturated Mixtures. *J. Chem. Eng. Data* **2010**, *55*, 4514–4520.

(25) Freire, M. G.; Neves, C. M. S. S.; Shimizu, K.; Bernardes, C. E. S.; Marrucho, I. M.; Coutinho, J. A. P.; Lopes, J. N. C.; Rebelo, L. P. N. Mutual Solubility of Water and Positional Isomers of *N*-Alkylpyridinium-Based Ionic Liquids. *J. Phys. Chem. B* **2010**, *114*, 15925–15934.

(26) Blesic, M.; Lopes, A.; Melo, E.; Petrovski, Z.; Plechkova, N. V.; Canongia Lopes, J. N.; Seddon, K. R.; Rebelo, L. P. N. On the Self-Aggregation and Fluorescence Quenching Aptitude of Surfactant Ionic Liquids. *J. Phys. Chem. B* **2008**, *112*, 8645–8650.

(27) Jorgensen, W. L.; McDonald, N. A. Development of an all-atom force field for heterocycles. Properties of liquid pyridine and diazenes. *J. Mol. Struct.: THEOCHEM* **1998**, *424*, 145–155.

(28) Canongia Lopes, J. N.; Deschamps, L.; Pádua, A. A. H. Modeling Ionic Liquids Using a Systematic All-Atom Force Field. *J. Phys. Chem. B* **2004**, *108*, 2038–2047.

(29) Canongia Lopes, J. N.; Pádua, A. A. H. Molecular force field for ionic liquids. III: Imidazolium, pyridinium and phosphonium cations; bromide and dicyanamide anions. *J. Phys. Chem. B* **2006**, *110*, 19586–19592.

(30) Freire, M. G.; Neves, C. M. S. S.; Shimizu, K.; Bernardes, C. E. S.; Marrucho, I. M.; Coutinho, J. A. P.; Canongia Lopes, J. N.; Rebelo, L. P. N. Mutual Solubility of Water and Structural/Positional Isomers of *N*-Alkylpyridinium-Based Ionic Liquids. *J. Phys. Chem. B* **2010**, *114*, 15925–15934.

(31) Smith, W.; Forester, T. R. The DL_POLY Package of Molecular Simulation Routines (v.2.17). The Council for The Central Laboratory of Research Councils; Daresbury Laboratory: Warrington, 2006.

(32) Zhang, S. J.; Sun, N.; He, X. Z.; Lu, X. M.; Zhang, X. P. Physical properties of ionic liquids: Database and evaluation. *J. Phys. Chem. Ref. Data* **2006**, *35*, 1475–1517.

(33) Rebelo, L. P. N.; Canongia Lopes, J. N.; Esperança, J. M. S. S.; Filipe, E. On the Critical Temperature, Normal Boiling Point, and Vapor Pressure of Ionic Liquids. *J. Phys. Chem. B* **2005**, *109*, 6040–6043.

(34) Earle, M. J.; Esperança, J. M. S. S.; Gilea, M. A.; Canongia Lopes, J. N.; Rebelo, L. P. N.; Magee, J. W.; Seddon, K. R.; Widegren, J. A. The Distillation and Volatility of Ionic Liquids. *Nature* **2006**, *439*, 831–834.

(35) Crosthwaite, J. M.; Muldoon, M. J.; Dixon, J. K.; Anderson, J. L.; Brennecke, J. F. Phase Transition and Decomposition Temperatures, Heat Capacities and Viscosities of Pyridinium Ionic Liquids. *J. Chem. Thermodyn.* **2005**, *37*, 559–568.

(36) Domalski, E. S.; Hearing, E. D. Heat Capacities and Entropies of Organic Compounds in the Condensed Phase, vol 3. *J. Phys. Chem. Ref. Data* **1996**, *25*, 1–525.

(37) Domanska, U.; Pobudkowska, A.; Eckert, F. Liquid-Liquid Equilibria in the Binary Systems (1,3-Dimethylimidazolium, or 1-Butyl-3-Methylimidazolium Methylsulfate plus Hydrocarbons). *Green Chem.* **2006**, *8*, 268–276.

(38) Domanska, U.; Marciniak, A. Solubility of 1-Alkyl-3-Methylimidazolium Hexafluorophosphate in Hydrocarbons. *J. Chem. Eng. Data* **2003**, *48*, 451–456.